

MODULATING THE ELECTRICAL PROPERTIES OF HEMATITE NANOSTRUCTURES WITH FUNCTIONALIZED CARBON NANOTUBES

S.A. GULUZHADADE, N.N. MUSAYEVA

*Azerbaijan Ministry of Science and Education, Institute of Physics,
H. Javid ave, 131, AZ1073, Baku, Azerbaijan*

This paper investigates the effect of functionalized carbon nanotubes (f-MWCNTs) on the electrical properties of nano-sized Hematite (Fe_2O_3) structures. Fe_2O_3 nanoparticles were synthesized using a simple sol-gel method, and 10 wt.% of f-MWCNTs were incorporated into this matrix with the assistance of ultrasound waves. The resulting nanocomposite was analyzed using XRD and FTIR spectroscopy methods. TEM analysis revealed that spherical nanoparticles were distributed on the carbon nanotubes, and decorating their surfaces. The electrical properties of Fe_2O_3 , f-MWCNTs, and Fe_2O_3 -f-MWCNTs nanocomposites were studied, and it was found that by adding a certain amount of f-MWCNTs to Fe_2O_3 using the above-described method, the electrical properties of the resulting nanocomposite were significantly improved.

Keywords: hematite, Fe_2O_3 , functionalized carbon nanotubes, sol-gel, nanoparticles

DOI:10.70784/azip.1.2025217

INTRODUCTION

Over the past few decades, numerous studies have focused on the investigation of the electrical and optical properties of nanostructured materials. These materials exhibit unique optical and electronic characteristics compared to bulk materials due to their strong absorption properties, large surface area, high porosity, and good permeability [8,9]. Research into these materials is valuable not only from a fundamental scientific perspective, but also due to their wide range of practical applications in everyday life. This is attributed to their distinctive electronic structure, chemical and mechanical stability, and their sensitivity to environmental conditions.

Transition metal oxides RuO_2 , MnO_2 , CuO , NiO , and Fe_2O_3 [10-15], which have excellent redox reversibility, high theoretical specific capacitance [10] were successfully applied in supercapacitors as electrodes [11,12], potential anode materials for Li-ion batteries, mainly due to their excellent stability and safety features [13]. From this point of view, NiO and Fe_2O_3 nanoparticles have attracted considerable attention. Fe_2O_3 is also attractive for its low cost, abundance, nontoxicity, and eco-friendliness [14,15].

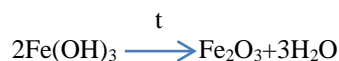
There are different ways of the synthesis of Fe_2O_3 NPs, such as spray pyrolysis [16,17], hydrothermal [18], and Sol-gel [19] methods. Both the synthesis methods and costs of the starting materials significantly influence the final material cost, which is crucial for the development and commercialization of the fabricated device.

When nanoxides are combined with carbon nanotubes to form composites, their electrical and optical properties are further enhanced. The high surface area and electrical conductivity of carbon nanotubes, when integrated with nanoxides, improve the material's electromagnetic characteristics and mechanical stability. These composites also offer new functional possibilities, enabling the development of more efficient materials for a wide range of applications.

In this work, we present a simple and cost-effective method for synthesizing Fe oxide nanoparticles (NPs). The resulting powdery nanomaterial was characterized using XRD, IR spectroscopy methods. To prepare the Fe_2O_3 -f-MWCNTs nanocomposite, an ultrasonication method was employed, and the final product was observed using TEM microscope. Electrical measurements were conducted at both room and elevated temperatures to study the electro-conductivity mechanism of the nanocomposite in its Ag- Fe_2O_3 -f-MWCNTs -Ag planar form structure.

EXPERIMENTAL

Iron oxide nanoparticles (Fe_2O_3) were synthesized using a simple sol-gel method. To begin, 0.1 M $\text{FeCl}_3 \cdot 6\text{H}_2\text{O}$ was dissolved in 100 ml of deionized water (Solution 1), and 5 M sodium hydroxide (NaOH) was dissolved in 16 ml of deionized water (Solution 2). Solution 1 was stirred at 1500 rpm with heating. Once the temperature of Solution 1 reached 90°C , Solution 2 was added dropwise over 1 hour, while maintaining constant magnetic stirring to keep the pH at 7. The mixture was stirred for an additional hour until the temperature decreased to 25°C . The resulting precipitate was collected by centrifugation, washed several times with deionized water to remove chloride and other unreacted ions, and then air-dried at 150°C . Finally, the samples were annealed at 300°C and 500°C for 3 hours in open air to convert $\text{Fe}(\text{OH})_3$ into dark reddish Fe_2O_3 nanoparticles, as shown in the following reaction:



All the samples were characterized using X-ray diffraction (XRD) to determine crystallinity, phase composition, and particle size. The analysis was performed with a D2 Phaser diffractometer from Bruker, utilizing $\text{CuK}\alpha$ radiation with a wavelength of 1.5406 \AA . Infrared (IR) spectroscopy was conducted using an IRAffinity-1 FTIR spectrometer from

Shimadzu, Japan, over the wavenumber range of 400–4000 cm^{-1} .

The MWCNTs were obtained from SWENT (USA) and have a purity of 98%. These MWCNTs were functionalized with oxygen-containing groups and analyzed. Further details can be found in our previously published articles [20, 21].

To prepare the Fe_2O_3 -f-MWCNTs nanocomposite, 10 wt.% of f-MWCNTs is taken relative to the dry Fe_2O_3 powder, and both compounds are mixed in a glass container with alcohol under the effect of ultrasonic waves for 1 hour, then they are dried again.

RESULTS AND DISCUSSION

X-ray diffraction analysis was conducted to determine the phase formation and crystallinity of the

Fe-O compound powder obtained at two different calcination temperatures. As shown in Fig. 1, improved crystallinity is achieved at 500°C. The prominent diffraction peaks correspond to the Standard JCPDS card no. 86-0550, confirming the crystallization of $\alpha\text{-Fe}_2\text{O}_3$ in the rhombohedral hexagonal phase. The additional small peaks are attributed to residual impurities. The average crystallite size was determined using Scherrer's formula:

$$L = \frac{k\lambda}{\beta \cos \theta},$$

where β is the full width at half maximum (FWHM). The calculated crystallite size is 10 nm. The crystallinity parameters and structure of the MWCNTs are discussed in our previous work [21].

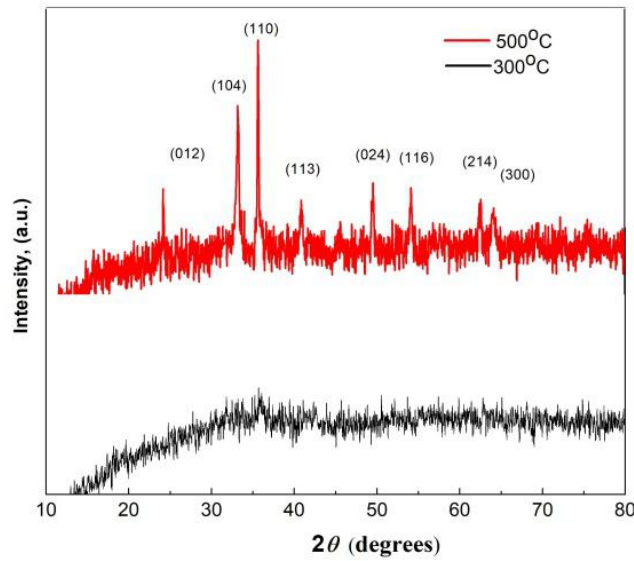


Fig. 1. X-ray pattern of $\alpha\text{-Fe}_2\text{O}_3$ NPs at different calcination temperatures.

IR spectroscopy analysis

Fig 2 shows comparative IR spectra of $\alpha\text{-Fe}_2\text{O}_3$, f-MWCNTs, and Fe_2O_3 -f-MWCNTs.

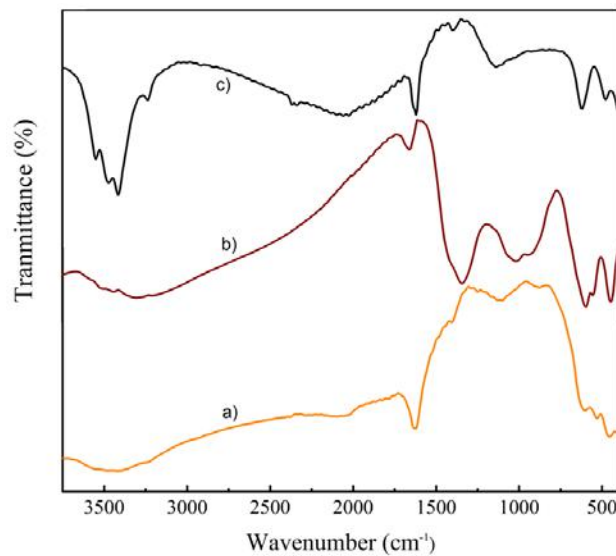


Fig. 2. IR spectra of a) $\alpha\text{-Fe}_2\text{O}_3$, b) f-MWCNTs, and c) Fe_2O_3 -f-MWCNTs. (The colour of the curves is selected similar to the material's colour).

In the FTIR spectrum of Fe₂O₃ (iron oxide), the peaks observed at 457, 530, 605, 878, 1627, and 3312 cm⁻¹ correspond to vibrations associated with Fe–O and O–H groups [22, 23]. The peak at 457 cm⁻¹ is related to the stretching vibration of Fe–O bonds, indicating the vibration of iron-oxygen bonds that are present in the main structure of Fe₂O₃. This wavelength represents the primary vibration of the Fe–O bonds in the crystal structure of Fe₂O₃. The peaks at 530 cm⁻¹ and 605 cm⁻¹ correspond to the stretching vibrations of other Fe–O bonds, representing different Fe–O bond interactions in the crystal structure of Fe₂O₃. These peaks may suggest the presence of different crystal forms of Fe₂O₃, such as the α-phase or a partially formed β-phase. The peak at 878 cm⁻¹ is related to the vibration of O–Fe–O bonds. The peak at 1627 cm⁻¹ is associated with the bending vibration of the O–H group, indicating the presence of hydroxyl groups or adsorbed water. The peak at 3312 cm⁻¹ is related to the stretching vibration of the O–H group, indicating the presence of water or hydroxyl groups on the surface of Fe₂O₃. These peaks provide important information about the Fe₂O₃ structure, including the nature of its iron-oxygen bonds and the presence of hydroxyl or water groups on the surface. When analyzing the FTIR spectrum of f-CNT, the peak at 480 cm⁻¹ is observed. This peak may represent the vibration of the primary carbon-carbon (C–C) bonds in the carbon nanotube. Additionally, this wavelength could sometimes indicate vibrations associated with metals (if the nanotube has been functionalized or incorporated into a composite material). The peak at 623 cm⁻¹ also indicates the vibration of C–C bonds. Peaks in the 3235, 3413, 3477, and 3550 cm⁻¹ range indicate the presence of hydroxyl groups. The peaks at 1145 cm⁻¹ and 1617 cm⁻¹ confirm the presence of carboxyl groups. The 1399 cm⁻¹ and 1617 cm⁻¹ ranges also suggest vibrations associated with the functionalization of the carbon nanotube [20, 21].

The FTIR spectrum of Fe₂O₃-f-MWCNTs differs (Some of the peaks of Fe₂O₃ is changed the position) from the spectra of the individual materials. The peaks observed at 450, 552, 596, 1016, 1345, 1405, 1661, and

3455 cm⁻¹ correspond to specific vibrational modes that arise from the interaction between Fe₂O₃ (iron oxide) and functionalized multi-walled carbon nanotubes (f-MWCNTs). The peaks at 450, 552, and 596 cm⁻¹ correspond to the Fe–O bond stretching vibration, which is characteristic of Fe₂O₃. It indicates the presence of iron-oxygen bonds within the iron oxide component of the composite. The peak at 1016 cm⁻¹ may correspond to the C–O stretching vibration, possibly related to the functional groups on the carbon nanotubes (such as hydroxyl or carboxyl groups) that were used for functionalization. The intensive peak, observed at 1345 cm⁻¹ is commonly attributed to the D-band of carbon nanotubes, which is associated with defects or disorder in the graphitic structure of the nanotubes. It was observed as a small peak on the curve of f-MWCNTs; however, the increased intensity may be attributed to Fe₂O₃ nanoparticles on the CNT surface, suggesting an increase in defects. 1405 cm⁻¹: This peak could be related to the C–O bending vibration or another defect-related vibration in the carbon nanotube structure. The peak 1661 cm⁻¹ is often seen in the C=C stretching region, which could indicate the presence of aromatic carbon-carbon bonds or graphitic structures within the carbon nanotubes. The broad peak at 3455 cm⁻¹ corresponds to the O–H stretching vibration, often associated with hydroxyl groups on the surface of the functionalized carbon nanotubes or adsorbed water.

TEM observation

Transmission Electron Microscopy (TEM) is a powerful technique used for high-resolution imaging of the internal structure and morphology of materials at the nanoscale. In this study, TEM observations were conducted to examine the detailed structural characteristics of the synthesized Fe₂O₃-f-MWCNTs composite. Fig 3 shows the distribution of Fe₂O₃ nanoparticles on the surface of functionalized multi-walled carbon nanotubes (f-MWCNTs).

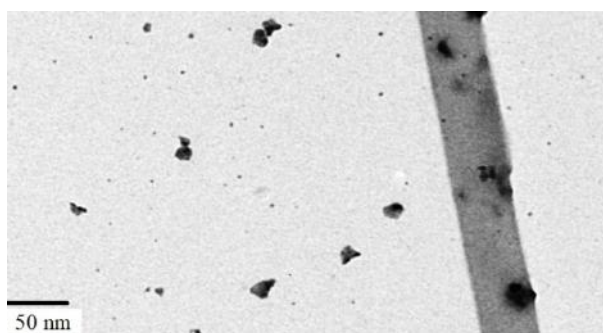


Fig. 3. TEM observation of individual MWCNT surface, which is decorated by Fe₂O₃ NPs

Electrical properties of Ag-Fe₂O₃-MWCNTs-Ag structure

To study the effect of carboxyl and hydroxyl group-functionalized MWCNTs on the electrical properties of Fe₂O₃, all three compositions were spin-

coated onto a polyceramic glass substrate in the form of thin layers. Electrical contacts were made using conductive Ag paste to create a planar contact. The current-voltage (I–V) characteristics of the samples were recorded at room temperature. Figure 1a shows the I–V curve for the Ag-Fe₂O₃-Ag structure.

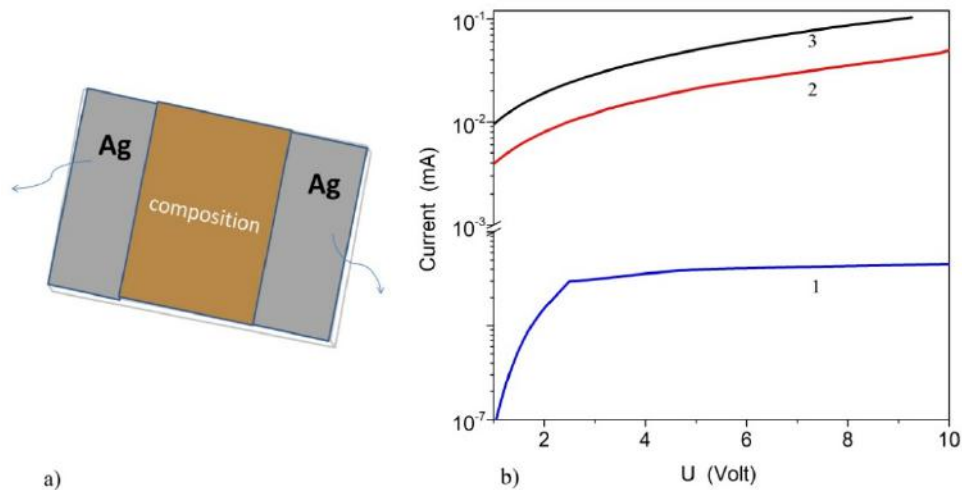


Fig.4. a) Sample structure of VAC experiments; Current –voltage characteristic curves of 1) Ag– Fe₂O₃; 2) Ag–f-MWCNTs and 3) Ag– Fe₂O₃–f-MWCNTs structures.

It is observed that in the sample with Ag paste contact on α -Fe₂O₃ (hematite), the current initially increases rapidly, but after approximately 2.4 Volts, it starts to change more slowly. This behavior suggests the formation of a Schottky barrier at the Ag/Fe₂O₃ interface. Due to the potential difference between the work function of silver (~4.3-4.7 eV) and the electronic structure of α -Fe₂O₃, the current increases sharply initially through tunneling and thermionic emission. As the voltage increases, this barrier saturates, and the rate of current increase slows down. This phenomenon is also attributed to the oxygen vacancies and defects present in Fe₂O₃. Additionally, at low voltages, surface conductivity predominates, but as the voltage increases, bulk conductivity also comes into play, and the rate of current increase slows down. Such a dependence is not observed in the I-V curves of the Ag f-M and Ag-Fe₂O₃/f-M CNT structures. Both structures show an ohmic region at low voltages, where the current increases linearly. However, as the voltage increases, the current starts to increase weakly in an exponential manner due to injection from the contacts.

From these observations, it can be concluded that the incorporation of functionalized CNTs into the Fe₂O₃ structure significantly affects its electrical conductivity. Unlike the Ag-Fe₂O₃ structure, the Ag-Fe₂O₃/f-MWCNTs structure exhibits more stable and controlled electrical conductivity. Such structures are considered promising for use as conductive layers in sensors and supercapacitors [22, 23].

CONCLUSION

This study investigated the impact of carboxyl and hydroxyl group-functionalized carbon nanotubes (CNTs) on the structural and electrical properties of Fe₂O₃. An optimal and cost-effective method for synthesizing Fe oxide nanoparticles was developed. X-ray diffraction analysis confirmed the formation of

α -Fe₂O₃, which crystallizes in a rhombohedral hexagonal phase. FTIR spectroscopy analysis of the prepared Fe₂O₃, functionalized multi-walled CNTs (f-MWCNTs), and Fe₂O₃/f-MWCNTs composites was conducted and compared. The results concluded that Fe₂O₃ predominantly adopts an alpha phase structure, with some beta-phase components present. The IR spectrum of Fe₂O₃/f-MWCNTs was distinct from those of Fe₂O₃ and f-MWCNTs, indicating that the combination of these structures may lead to the formation of a new composite material with enhanced properties. The findings also revealed that the Ag-Fe₂O₃ system exhibited a Schottky barrier at the Ag/Fe₂O₃ interface, causing a rapid increase in current at low voltages, followed by a slowing of current growth due to barrier saturation. This behavior was influenced by oxygen vacancies and defects in Fe₂O₃, as well as the transition from surface to bulk conductivity. In contrast, the Ag-Fe₂O₃/f-MWCNTs composite demonstrated more stable electrical characteristics. The presence of CNTs facilitated a more controlled and linear increase in current at low voltages, while exponential current growth was observed at higher voltages due to charge injection. These results suggest that the functionalization of CNTs significantly enhances the electrical properties of Fe₂O₃, thereby improving its overall performance. The incorporation of functionalized CNTs into Fe₂O₃ led to a notable improvement in both the material's conductivity and stability. Unlike the traditional Ag-Fe₂O₃ structure, the Ag-Fe₂O₃/f-MWCNTs composite exhibited more consistent and reliable electrical behavior. These results highlight the potential of functionalized CNTs to optimize the electrical properties of composite materials, opening the door for future applications in advanced electronic devices and energy storage systems.

[1] M. Ghadiriy, M. Gholami, L. Choon Kong, C. Wu Yi, H. Ahmad, Y. Alias. Nano-Anatase TiO₂ for High Performance Optical Humidity

Sensing on Chip. *Sensors* 2016, 16, 39. <https://doi.org/10.3390/s16010039>, [2] Halima Ghorbel, Luc Damé, Mustapha Meftah,

- Xavier Arrateig, Faustine Bouyssou, et al. Preparation and Characterization of β -Ga₂O₃-based Photo detectors for UV Detection Applications. 7th International Conference on Sensors Engineering and Electronics Instrumentation Advances (SEIA' 2021), Sep 2021, Palma de Mallorca, Spain.
- [3] C. Wang, L. Yin, L. Zhang, D. Xiang, R. Gao. Metal Oxide Gas Sensors: Sensitivity and Influencing Factors. *Sensors* 2010, 10, 2088–2106. <http://dx.doi.org/10.3390/s100302088>
- [4] K. Wetchakuna, T. Samerjai, N. Tamaekonga, C. Liewhirana, C. Siriwonga, V. Kruefua, A. Wisitsoraat, A. Tuantranont, S. Phanichphant. Semiconducting metal oxides as sensors for environmentally hazardous gases. *Sens. Actuators* 2011, 160, 580–591. [CrossRef]
- [5] R. Dhahri, M. Hjiri, L. El Mir, H. Alamri, A. Bonavita, D. Iannazzo, S.G. Leonardi, G. Neri. CO sensing characteristics of In-doped ZnO semiconductor nanoparticles, *Journal of Science: Advanced Materials and Devices* 2(2017) 34-40, <http://dx.doi.org/10.1016/j.jsamd.2017.01.003>
- [6] N.V. Duy, N.V. Hieu, P.T. Huy, N.D. Chien, M. Thamilselvan, & J. Yi. (2008). Mixed SnO₂/TiO₂ included with carbon nanotubes for gas-sensing application. *Physica E: Low-Dimensional Systems and Nanostructures*, 41(2), 258–263. <https://doi.org/10.1016/J.PHYSE.2008.07.007>
- [7] N.H. Khadry, A.S. Alayyar, L.M. Alsarhan, S. Alshihri, M. Mokhtar. Metal Oxides as Catalyst/Supporter for CO₂ Capture and Conversion, Review. *Catalysts* 2022, 12, 300. <https://doi.org/10.3390/catal12030300>
- [8] H. Kim, M.-C. Kim, S. Kim, Y.-S. Kim, J.-H. Choi, & K.-W. Park. *RSC Advances* 2020, v.10 (18), p.10519. <https://doi.org/10.1039/D0RA00531B>
- [9] Y. Zou, S. Chen, J. Sun, J. Liu, Y. Che, X. Liu, D. Yang. *ACS Sensors* 2017, v. 2 (7), p. 897. <https://doi.org/10.1021/acssensors.7b00276>
- [10] X. Zhang, W. Shi, J. Zhu, W. Zhao, J. Ma, S. Mhaisalkar, T.L. Maria, Y. Yang, H. Zhang, H.H. Hng, Q. Yan. Synthesis of porous NiO nanocrystals with controllable surface area and their application as supercapacitor electrodes, *Nano Res.* 3 (2010) 643–652. <https://doi.org/s12274-010-0024-6>
- [11] A. Roy, A. Ray, S. Saha, M. Ghosh, T. Das, B. Satpati, M. Nandi, S. Das. NiO-CNT composite for high performance supercapacitor electrode and oxygen evolution reaction, *Electrochimica Acta* (2018), <https://doi.org/10.1016/j.electacta.2018.06.154>
- [12] S. Zhang, X. Wang, Y. Li, X. Mu, Y. Zhang, J. Du, G. Liu, X. Hua, Y. Sheng, E. Xie, Zhang, Z. Beilstein. *J. Nanotechnol.* 2019, 10, 1923–1932. [doi:10.3762/bjnano.10.188](https://doi.org/10.3762/bjnano.10.188)
- [13] H. Kim, S.-M. Oh, B. Scrosati, Y.-K. Sun. 9-High-performance electrode materials for lithium-ion batteries for electric vehicles, *Woodhead Publishing Series in Energy*, 2015, Pages 191-241 <https://doi.org/10.1016/B978-1-78242-377-5.00009-1>
- [14] T. Li, H. Yu, L. Zhi, W. Zhang, L. Dang, Z. Liu, Z. Lei. Facile Electrochemical Fabrication of Porous Fe₂O₃ Nanosheets for Flexible Asymmetric Supercapacitors. *J. Phys. Chem. C* 2017, 121, 18982–18991. <https://doi.org/10.1021/acs.jpcc.7b04330>
- [15] Z. Zhang, H. Wang, Y. Zhang, X. Mu, B. Huang, J. Du, J. Zhou, X. Pan, E. Xie. *Chem. Eng. J.* 2017, 325, 221–228. <https://doi.org/10.1016/j.cej.2017.05.045>
- [16] P.S. Patil, L.D. Kadam. Preparation and characterization of spray pyrolyzed nickel oxide (NiO) thin films, *Applied Surface Science*, Volume 199, Issues 1–4, 2002, Pages 211-221, [https://doi.org/10.1016/S0169-4332\(02\)00839-5](https://doi.org/10.1016/S0169-4332(02)00839-5)
- [17] Rich Kant, Dinesh Kumar and Viresh Dutta. High coercivity α -Fe₂O₃ nanoparticles prepared by continuous spray pyrolysis *RSC Adv.*, 2015, 5, 52945-52951
- [18] Kiyamu Sue, Shin-ichiro Kawasaki, Muneyuki Suzuki, Yukiya Hakuta, Hiromichi Hayashi, Kunio Arai, Yoshihiro Takebayashi, Satoshi Yoda, Takeshi Furuya. Continuous hydrothermal synthesis of Fe₂O₃, NiO, and CuO nanoparticles by superrapid heating using a T-type micro mixer at 673K and 30MPa, *Chemical Engineering Journal*, Volume 166, Issue 3, 2011, Pages 947-953, <https://doi.org/10.1016/j.cej.2010.11.080>
- [19] K. Raja, M. Mary Jaculine, M. Jose, Sunil Verma, A.A.M. Prince, K. Ilangoan, K. Sethusankar, S. Jerome Das, Sol-gel synthesis and characterization of α -Fe₂O₃ nanoparticles, *Superlattices and Microstructures*, Volume 86, 2015, Pages 306-312, <https://doi.org/10.1016/j.spmi.2015.07.044>
- [20] M. Koç, F. Tatardar, N. Musayeva, S. Guluzade, A. Sari, L. Paralı. The piezoelectric properties of three-phase electrospun PVDF/PZT/Multiwalled Carbon Nanotube composites for energy harvesting applications. *Journal of Alloys and Compounds* 1003, 175578, (2024). <https://doi.org/10.1016/j.jallcom.2024.175578>
- [21] S. Guluzade, N. Musayeva. Room temperature detection of sulfur dioxide using functionalized carbon nanotubes. *Digest Journal of Nanomaterials and Biostructures*, 2023, v.18, 4, pp1363-1370
- [22] M. Dutt, K. Suhasini, A. Ratan, J. Shah, R.K. Kotnala, & V. Singh. 2018. Mesoporous silica mediated synthesis of α -Fe₂O₃ porous structures and their application as humidity sensors. *Journal of Materials Science: Materials in Electronics*. doi:10.1007/s10854-018-0186-7
- [23] Y. Du, H. Fan, L. Wang, J. Wang, J. Wu, & H. Dai. 2013. α -Fe₂O₃ nanowires deposited diatomite: highly efficient absorbents for the

- removal of arsenic. *Journal of Materials Chemistry A*, 1(26), 7729.
doi:10.1039/c3ta11124e
- [24] *D. Zheng, Ch. Sun, et.al.* Nanostructured Fe₂O₃@C Negative Electrodes for Stable Asymmetric Supercapacitors with High-Performance. *Energy Fuels* 2021, 35, 20, 16915–16924, <https://doi.org/10.1021/acs.energyfuels.1c02581>

Received: 02.04.2025